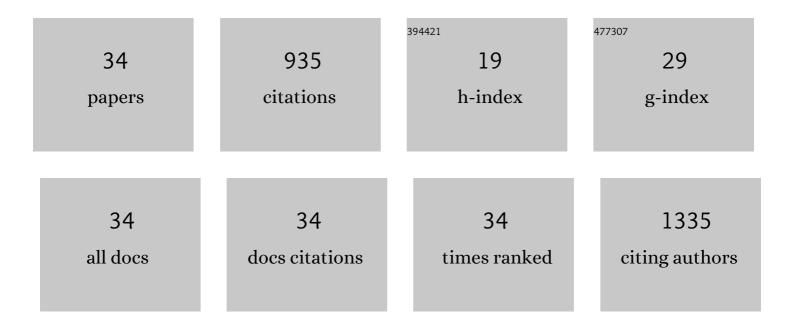
## Pu Duan

## List of Publications by Year in descending order

Source: https://exaly.com/author-pdf/5934534/publications.pdf Version: 2024-02-01



ΡΗ ΠΗΛΝ

#	Article	IF	CITATIONS
1	Binding Sites of a Positron Emission Tomography Imaging Agent in Alzheimer's β-Amyloid Fibrils Studied Using <sup>19</sup> F Solid-State NMR. Journal of the American Chemical Society, 2022, 144, 1416-1430.	13.7	22
2	Fluent molecular mixing of Tau isoforms in Alzheimer's disease neurofibrillary tangles. Nature Communications, 2022, 13, .	12.8	27
3	Inclusion of the C-Terminal Domain in the β-Sheet Core of Heparin-Fibrillized Three-Repeat Tau Protein Revealed by Solid-State Nuclear Magnetic Resonance Spectroscopy. Journal of the American Chemical Society, 2021, 143, 7839-7851.	13.7	30
4	Structurally Based Design of Glucagon Mutants That Inhibit Fibril Formation. Biochemistry, 2021, 60, 2033-2043.	2.5	4
5	Xylan Structure and Dynamics in Native <i>Brachypodium</i> Grass Cell Walls Investigated by Solid-State NMR Spectroscopy. ACS Omega, 2021, 6, 15460-15471.	3.5	19
6	Physicochemical Changes in Biomass Chars by Thermal Oxidation or Ambient Weathering and Their Impacts on Sorption of a Hydrophobic and a Cationic Compound. Environmental Science & Technology, 2021, 55, 13072-13081.	10.0	7
7	Structural composition of immobilized fertilizer N associated with decomposed wheat straw residues using advanced nuclear magnetic resonance spectroscopy combined with 13C and 15N labeling. Geoderma, 2021, 398, 115110.	5.1	5
8	A New Method for Solid Acid Catalyst Evaluation for Cellulose Hydrolysis. Sustainable Chemistry, 2021, 2, 645-669.	4.7	4
9	A molecular fluorophore in citric acid/ethylenediamine carbon dots identified and quantified by multinuclear solidâ€state nuclear magnetic resonance. Magnetic Resonance in Chemistry, 2020, 58, 1130-1138.	1.9	34
10	Quantifying Molecular Mixing and Heterogeneity in Pharmaceutical Dispersions at Sub-100 nm Resolution by Spin Diffusion NMR. Molecular Pharmaceutics, 2020, 17, 3567-3580.	4.6	26
11	Hydration and Dynamics of Full-Length Tau Amyloid Fibrils Investigated by Solid-State Nuclear Magnetic Resonance. Biochemistry, 2020, 59, 2237-2248.	2.5	30
12	Rapid Depolymerization of Decrystallized Cellulose to Soluble Products via Ethanolysis under Mild Conditions. ChemSusChem, 2020, 13, 2634-2641.	6.8	7
13	Multinuclear solid-state NMR of complex nitrogen-rich polymeric microcapsules: Weight fractions, spectral editing, component mixing, and persistent radicals. Solid State Nuclear Magnetic Resonance, 2020, 106, 101650.	2.3	3
14	Structure of the Polymer Backbones in polyMOF Materials. Journal of the American Chemical Society, 2020, 142, 10863-10868.	13.7	19
15	Effects of post-pyrolysis air oxidation on the chemical composition of biomass chars investigated by solid-state nuclear magnetic resonance spectroscopy. Carbon, 2019, 153, 173-178.	10.3	10
16	Synthesis and Reactivity of Zr MOFs Assembled from P <sup>N</sup> N <sup>N</sup> P-Ru Pincer Complexes. Organometallics, 2019, 38, 3419-3428.	2.3	14
17	Silk-Like Protein with Persistent Radicals Identified in Oyster Adhesive by Solid-State NMR. ACS Applied Bio Materials, 2019, 2, 2840-2852.	4.6	8
18	Phase transition of spiropyrans: impact of isomerization dynamics at high temperatures. Chemical Communications, 2019, 55, 5813-5816.	4.1	17

Pu Duan

#	Article	IF	CITATIONS
19	Quick, selective NMR spectra of C OH moieties in 13C-enriched solids. Journal of Magnetic Resonance, 2019, 301, 80-84.	2.1	5
20	Polymer Infiltration into Metal–Organic Frameworks in Mixed-Matrix Membranes Detected in Situ by NMR. Journal of the American Chemical Society, 2019, 141, 7589-7595.	13.7	102
21	Postsynthetic Metal Exchange in a Metal–Organic Framework Assembled from Co(III) Diphosphine Pincer Complexes. Inorganic Chemistry, 2019, 58, 3227-3236.	4.0	23
22	Reaction engineering implications of cellulose crystallinity and water-promoted recrystallization. Green Chemistry, 2019, 21, 5541-5555.	9.0	40
23	Zirconium Metal–Organic Frameworks Assembled from Pd and Pt P <sup>N</sup> N <sup>N</sup> P Pincer Complexes: Synthesis, Postsynthetic Modification, and Lewis Acid Catalysis. Inorganic Chemistry, 2018, 57, 2663-2672.	4.0	29
24	Cellulase-Inspired Solid Acids for Cellulose Hydrolysis: Structural Explanations for High Catalytic Activity. ACS Catalysis, 2018, 8, 1464-1468.	11.2	40
25	Stability of Pd nanoparticles on carbon-coated supports under hydrothermal conditions. Catalysis Science and Technology, 2018, 8, 1151-1160.	4.1	28
26	Carbon Nitride Nanothread Crystals Derived from Pyridine. Journal of the American Chemical Society, 2018, 140, 4969-4972.	13.7	81
27	The Chemical Structure of Carbon Nanothreads Analyzed by Advanced Solid-State NMR. Journal of the American Chemical Society, 2018, 140, 7658-7666.	13.7	59
28	Constraining Carbon Nanothread Structures by Experimental and Calculated Nuclear Magnetic Resonance Spectra. Nano Letters, 2018, 18, 4934-4942.	9.1	24
29	Protective Carbon Overlayers from 2,3-Naphthalenediol Pyrolysis on Mesoporous SiO2 and Al2O3 Analyzed by Solid-State NMR. Materials, 2018, 11, 980.	2.9	4
30	Improved hydrothermal stability of Pd nanoparticles on nitrogen-doped carbon supports. Catalysis Science and Technology, 2018, 8, 3548-3561.	4.1	20
31	A Major Step in Opening the Black Box of High-Molecular-Weight Dissolved Organic Nitrogen by Isotopic Labeling ofSynechococcusand Multibond Two-Dimensional NMR. Analytical Chemistry, 2017, 89, 11990-11998.	6.5	12
32	Deactivation of Supported Pt Catalysts during Alcohol Oxidation Elucidated by Spectroscopic and Kinetic Analyses. ACS Catalysis, 2017, 7, 6745-6756.	11.2	33
33	Composite-pulse and partially dipolar dephased multiCP for improved quantitative solid-state 13 C NMR. Journal of Magnetic Resonance, 2017, 285, 68-78.	2.1	61
34	Carbon Overcoating of Supported Metal Catalysts for Improved Hydrothermal Stability. ACS Catalysis, 2015, 5, 4546-4555.	11.2	88